JOURNAL OF AIRCRAFT
Vol. 42, No. 4, July–August 2005

# Sting Effects on Store Captive Loads

L. Y. Jiang,* F. C. Tang,† A. Benmeddour,‡ and F. Fortin‡
*National Research Council Canada, Ottawa, Ontario K1A 0R6, Canada*

**An articulated sting is a key device used at the Institute for Aerospace Research 1.5m Trisonic Blowdown Wind Tunnel for store loads measurements in an aircraft flowfield. The effects of the articulated sting on the captive loads of the MK83-BSU mounted on a 6% scale CF-18 model were investigated at different transonic Mach numbers, aircraft angles of attack, and aircraft/stores configurations. In this paper, the sting-induced increments in store captive loads at Mach numbers 0.6, 0.85, and 0.95 are discussed and qualitatively verified by the computational solutions from an Euler code. The influence of Mach number on sting-induced increments is complicated at transonic speeds, and the induced increment may not monotonically decrease with increasing Mach number. A detailed analysis is needed for each individual case if the accurate sting effects are required. The sting effects on the store trajectories released from the CF-18 are also studied. It is found that for the store safety release errors because of sting effects are negligible for the conditions investigated.**

## Introduction

THE importance of understanding the model support interference on wind-tunnel test data has long been recognized. This is especially true in wind-tunnel stores work, as the store model size is often comparable to that of the support sting.

Much effort has been devoted to studying this subject.[1] Sting effects on aerodynamic loads of bodies of revolution were experimentally studied at different Mach-number regimes by many investigators.[2–4] Stings with varying diameter, cone angle, and cylindrical length were employed in these studies, and some guidelines for minimizing sting interference were given. A series of wind-tunnel tests were conducted at Arnold Engineering Development Center to evaluate the effects of their captive trajectory dual-sting system (CTS) on store captive loads.[5] Measurements were made of the aerodynamic loads acting on eight different stores externally mounted at various positions on a 5% scale F-4C aircraft model. In these tests, the store support sting of the CTS was used as a dummy sting, and store captive loads were measured by internal triple ejection rack (TER) or pylon balances. An aircraft angle-of-attack range from −4 to 10 deg and a Mach-number range of 0.6 to 1.2 were covered. It was found that sting-induced loads were a function of angle of attack, Mach number, position in the aircraft flowfield, and ratio of the sting diameter to the store base diameter. The presence of a sting influenced pitching and yawing moments more than other load components, and the influence generally decreased with increasing Mach number. More recently, Cenko and his coworkers[6] experimentally investigated the CTS sting effects on the captive loads of a standoff missile mounted on a F-18 outboard pylon at high transonic speeds and compared these data with the numerical solutions obtained from two computational codes. They found that the sting effects could significantly compromise the CTS measured store aerodynamic loads and thus lead to a wrong solution regarding store safety release at the certain test conditions.

To evaluate the effects of a grid survey system on store loads measurements, a research program was initiated at Institute for Aerospace Research (IAR). The MK83-BSU was chosen as a test store because its wind-tunnel data were comprehensive. In addition, the ratio of the diameter of the sting end to the store base diameter was large, 0.95, and the sting induced-increments in store loads were expected to be more noticeable. This represents one of the critical cases in the store wind-tunnel loads measurements at IAR. In this paper, the wind-tunnel investigation is outlined, and some of the results are presented. Analyses of these results are supplemented by the numerical solutions obtained from an Euler code. Finally, the separation trajectories computed of the MK83-BSU released from the CF-18 with and without the sting effects are discussed.

## Wind-Tunnel Investigation of Sting Effect

### Wind-Tunnel Setup

The investigation was performed at the transonic test section of the IAR 1.5m Trisonic Blowdown Wind Tunnel.[7] It has a Mach-number range of 0.1 to 4.2 and can be operated over a range of stagnation pressures to maintain a constant Reynolds number for different Mach numbers. The grid survey system used for store loads measurements within a parent aircraft flowfield is shown in Fig. 1. A rigid 6% scale model of the CF-18 was supported on a 3.81-cm (1.5-in.)-diam dummy balance attached to a roof-mounted strut. The aircraft model, shown in Fig. 2, is equipped with 10 infrared-emitting diodes (IREDs) embedded in the starboard side of the forebody. These IREDs are used to accurately define the location and attitude of the aircraft model through an optical tracking system OPTOTRAK/3020 (Ref. 8). For this study, AIM-9 and AIM-7 missiles were mounted on the wing tips and fuselage stations respectively. All flaps and stabilators were set to 0 deg.

The articulated sting is the key device used in the IAR 1.5m Trisonic Blowdown Wind Tunnel for store loads measurements. As shown in Fig. 1, the articulated sting is installed on the wind-tunnel main strut. It can be moved vertically 63.5 cm (25 in.) below and 25.4 cm (10 in.) above the tunnel center line, and its effective horizontal traverse is 40.7 cm (16 in.). The sting lateral position is determined by the angular positions of the radial arms of the articulated sting. The sting roll position is adjusted by rotating an extending shaft. A 36-conductor cable inside the articulated sting carries electrical power and signals to and from the measurement device.

For the present investigation, the articulated sting was used as a dummy sting with a cylindrical extension attached to its upstream end. The extension, 1.27 cm (0.5 in.) in diameter and 3.81 cm (1.5 in.) long, was instrumented with six IREDs. This arrangement enabled the optical tracking system to accurately detect the position and attitude of the sting extension relative to the metric store during wind-on operation.

Presented as Paper 2001-0575 at the AIAA 39th Aerospace Sciences Meeting & Exhibit, Reno, NV; received 5 April 2004; revision received 21 July 2004; accepted for publication 21 July 2004. 

*Research Officer, 1200 Montreal Road, Aerodynamics Laboratory, Institute for Aerospace Research; leiyong.jiang@nrc-cnrc.gc.ca.
†Senior Research Officer, 1200 Montreal Road.
‡Research Officer, 1200 Montreal Road, Aerodynamics Laboratory, Institute for Aerospace Research.

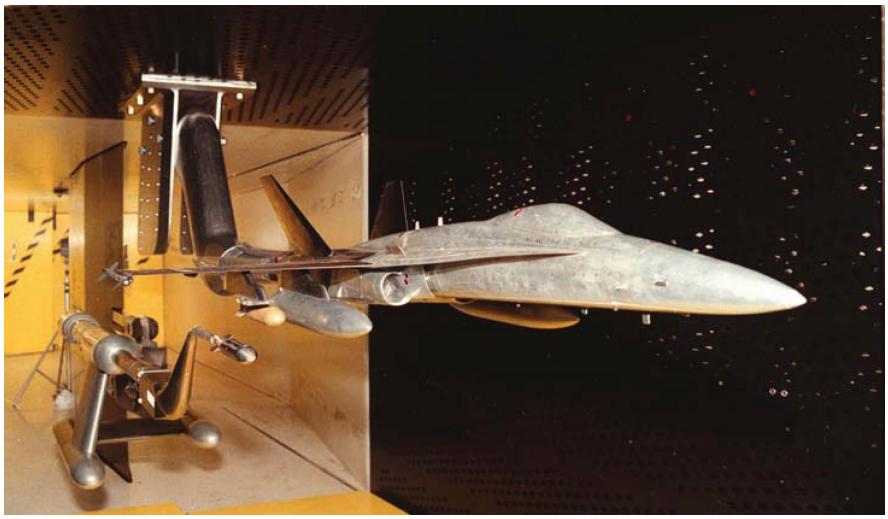

**Fig. 1 Grid survey system at IAR.**

**Fig. 2 6% scale CF-18 W/T model.**

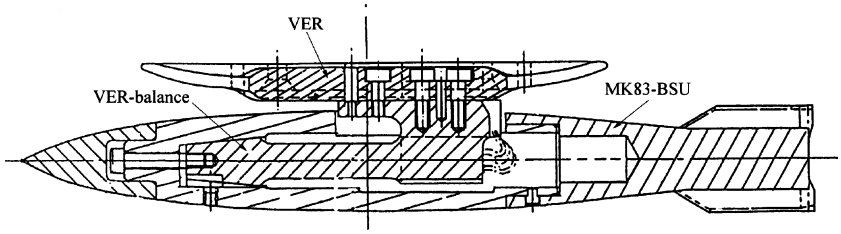


**Fig. 3 Assembly of metric MK83-BSU, VER, and VER balance.**

### Metric MK83-BSU and Instrumentation

A 6% scale metric model of the MK83-BSU is schematically shown in Fig. 3 together with a vertical ejection rack (VER) and a five-component VER balance. The model consists of three removable pieces: a nose, a centerbody, and a tail section. The diameter of the tail cylindrical body is 13.386 mm (0.527 in.). The upper surface of the centerbody is cut to allow installation of the VER balance. The clearance between the offset arm of the VER balance and the centerbody is 0.508 mm (0.02 in.) in the lateral direction and 1.27 mm (0.05 in.) in the axial direction. These clearances allow unrestricted reaction of the VER balance to store aerodynamic loads.

The position and attitude of the sting extension relative to the MK83-BSU metric store were measured by the optical tracking system OPTOTRAK/3020. IREDs embedded in the CF-18 model, the sting extension, and the wind-tunnel wall emitted infrared strobe signals when activated. Two charge-coupled-device cameras were responsible for sensing these strobe signals. With information from the cameras, the positions and attitudes of the sting extension with respect to the wind-tunnel reference frame, the CF-18 aircraft, and the metric store were determined at a rate of 100 Hz.

### Test Program

The sting effects on MK83-BSU captive loads were measured at Mach numbers 0.6, 0.85, and 0.95, and aircraft angles of attack (AOA) 0, 2, and 4 deg. A nominal Reynolds number of $6.2 \times 10^6$/ft gave sufficient run time to accomplish the required measurements. The three CF-18 aircraft/stores configurations tested are shown in Fig. 4. For configuration A, four MK83-BSU stores were mounted on each side of the CF-18, and the articulated sting was located behind the most outboard store on the port wing. For configurations B and C, 330-gall fuel tanks were mounted on inboard pylons, and the sting was behind the outboard and inboard MK83-BSU of the port outboard VER, respectively.

The programmed travel path of the sting extension is illustrated in Fig. 5. The sting extension moved along the store axis of symmetry

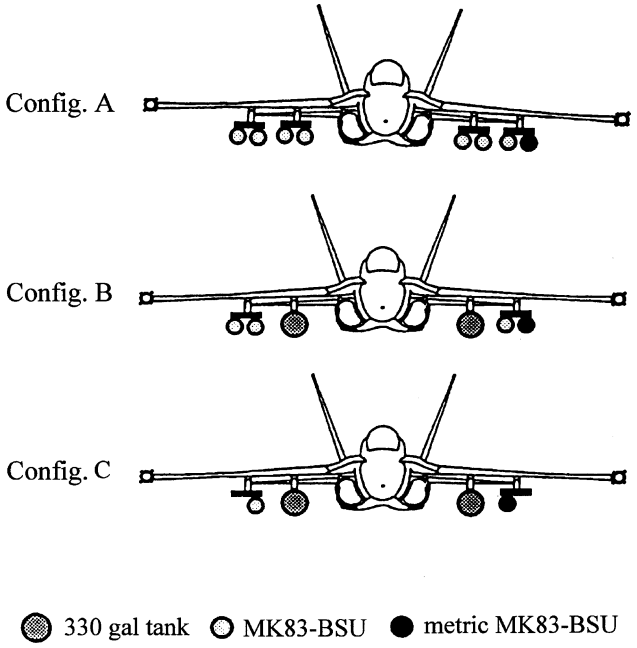


**Fig. 4 CF-18/stores configurations.**

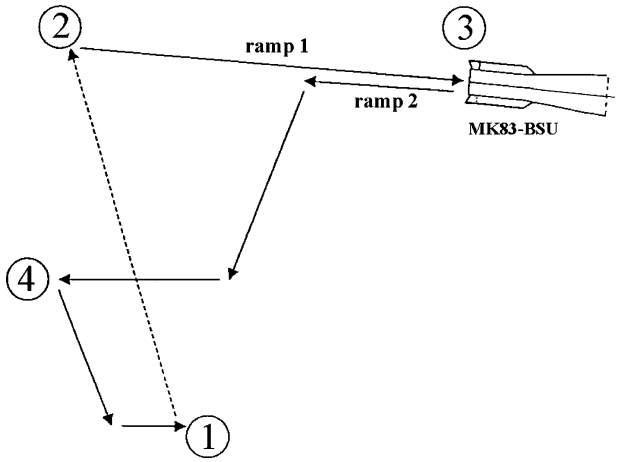


**Fig. 5 Travel path of the articulated sting extension.**

at a speed of 0.1778 m/s (0.7 in./s) or 0.0508 m/s (0.2 in./s), and the captive loads of the metric store were measured by the VER balance at a sampling rate of 100 Hz. Measurements were also made at points 1, 3, and 4 as the sting paused at these points. Point 1 was about 25.4 cm (10 in.) below and 12.7 cm (5 in.) behind the store reference point (the center of the base surface), and point 4 was approximately 17.78 cm (7 in.) away from the reference point in both vertical and horizontal directions.

Effort was made to align the sting extension with the metric model axis of symmetry. The minimum axial distance between the sting extension and the store reference point (at point 3) was less than 1.27 mm (0.05 in.) for most of the runs, and the misalignment in both lateral and vertical directions was less than 1.27 mm (0.05 in.). Runs with misalignment greater than 1.27 mm (0.05 in.) were discarded.

Because of a slight misalignment in the vertical or lateral direction, a small forward-facing step over a portion of the store base might occur. Because the flowfield around the store was dominated by the parent aircraft and the maximum size of the forward-facing step was 7% of the store base diameter, it is believed that the flow characteristics over the tail portion of the store would not change and the effect on the store loads was insignificant.

### Accuracy of Data

For subsonic and transonic testing at the IAR 1.5m Trisonic Blowdown Wind Tunnel, a computerized control system sets the desired test-section Mach number to an accuracy of $\pm 0.003$. Typical dynamic pressure uncertainty is $\pm 0.207$ kPa ($\pm 0.03$ psia) for a run Mach number of 0.6 at a stagnation pressure of 178.58 kPa (25.9 psia). Balance uncertainty was checked by reconstruction of the applied calibrating loads using the signals generated and the deduced linear matrix. The positional accuracy of the optical tracking system is $\pm 0.254$ mm ($\pm 0.01$ in.) in axial and lateral direction and $\pm 0.127$ mm ($\pm 0.005$ in.) in vertical direction. The angular accuracy is $\pm 0.25$ deg in pitch and yaw and about $\pm 1$ deg in roll.

## Results and Discussion

### Wind-Tunnel Results

Results for configuration C at AOA $= 2$ deg, $M = 0.6$, 0.85, and 0.95 are discussed in this paper. As shown in Fig. 6, the MK83-BSU captive loads vary with the axial position of the sting extension relative to the store reference point at $M = 0.6$. Because the rolling moment is insensitive to the presence of a sting, it is not included in the presentation. Hollow circles denote store captive loads measured when the sting extension moved towards the store along the store axis of symmetry. Solid circles stand for store captive loads obtained as the sting extension paused at points 1, 3, and 4. Note that points 1 and 4 are not in the same travel path as other data points. They are far below the store axis of symmetry (see Fig. 5).

As the sting extension travels towards the store from 17.78 cm (7 in.) behind, the store captive loads vary slowly. However, as the sting extension is about 2.54 cm (1 in.) away from the store, the store captive loads start to change rapidly and reach their peaks at about 0.508 cm (0.2 in.) to the store reference point. Rapid recovery from the peak values is observed as the sting extension moves closer towards the metric store. These observations indicate that the store base-flow structure varies dramatically as the sting extension travels in the vicinity of the store. It is understood that as the sting extension is far enough from the store a large flow separation region occurs immediately behind the store base. As the sting approaches the store base surface ($<1.27$ mm or 0.05 in.), the large separation region disappears. Between these two extreme cases, the flow behind the store can exhibit complicated behavior.

At point 3, as mentioned earlier, the sting extension nearly touches the store base surface. Therefore, the measured store captive loads at this position can be considered as the store captive loads with the articulated sting attached. Points 1 and 4 are far away from the metric store and aircraft model, and hence data obtained at these locations can be treated as the store captive loads without the sting effects. By comparing loads at point 3 with those at points 1 and 4, the sting effects on store captive loads can be assessed.

In general, with the sting attached to the store base, the pressure on the aft portion of the store would increase slightly as a result of a decrease in flow acceleration. The resulting normal force on the aft portion of the store depends on the flow conditions over the upper and lower surfaces of the store. For the case discussed in Fig. 6, the upward normal-force coefficient ($C_Z$, positive downward) is reduced by 0.05 as a result of the presence of the sting (see the store loads at point 3 and those at points 1 and 4). Less upward normal force acting on the aft portion of the store results in an increase in pitching moment (positive nose up). This is consistent with the wind-tunnel data as shown in Fig. 6, where the store captive pitching moment $C_m$ is increased by 0.13.

From the previous CF-18 flowfield survey,[8] it is known that the external fuel tank mounted on the inboard pylon together with the fuselage and wing creates large sidewash at the outboard weapon station. The crossflow acceleration over the store base region would be reduced because of the presence of the sting. Consequently, the pressure distribution on the inboard and outboard surfaces of the aft portion of the store would be modified. The resulting effect is shown in Fig. 6. The inward side-force coefficient ($C_Y$, positive outward) is reduced by 0.03. A decrease in inward side force over the store aft portion causes the store yawing moment (positive nose outward) to decrease. This agrees with the measured result in Fig. 6, where the yawing-moment coefficient $C_n$ shows a decrease of 0.13.

In Fig. 7, the MK83-BSU captive loads vs the axial distance between the sting extension and the store at $M = 0.85$ are illustrated.

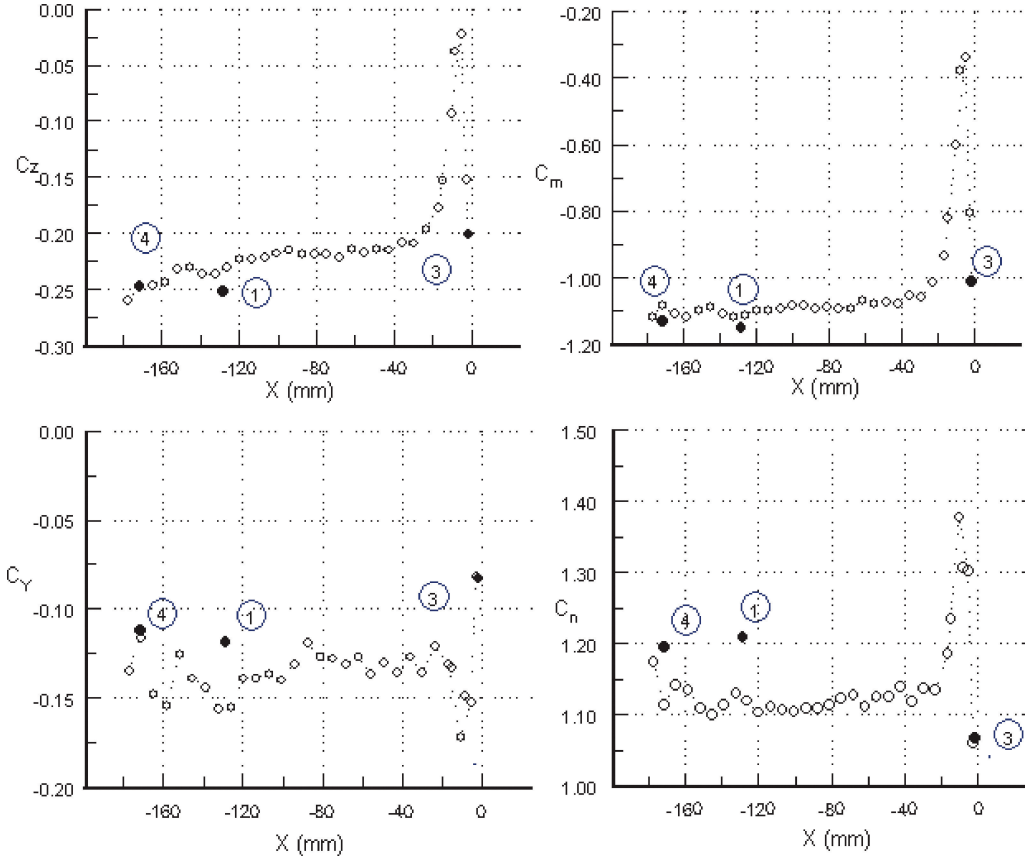


**Fig. 6 MK83-BSU carriage loads for configuration C: $M = 0.6$ and AOA = 2 deg.**

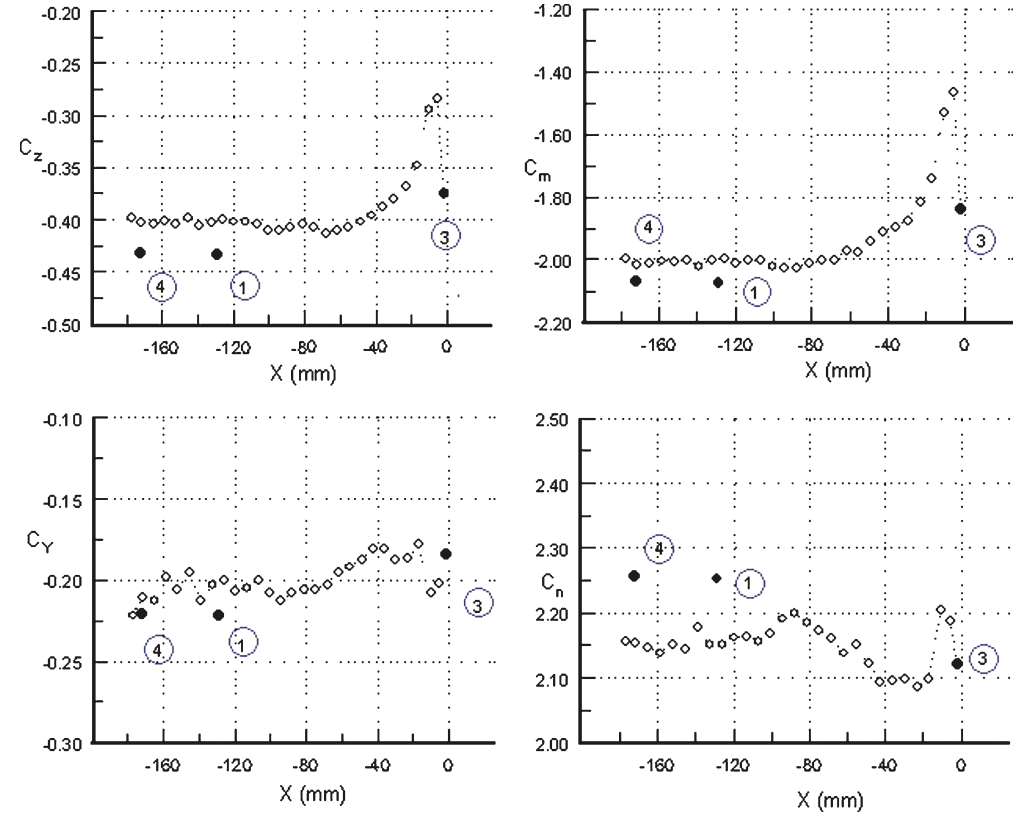


**Fig. 7 MK83-BSU carriage loads for configuration C: $M = 0.85$ and AOA = 2 deg.**

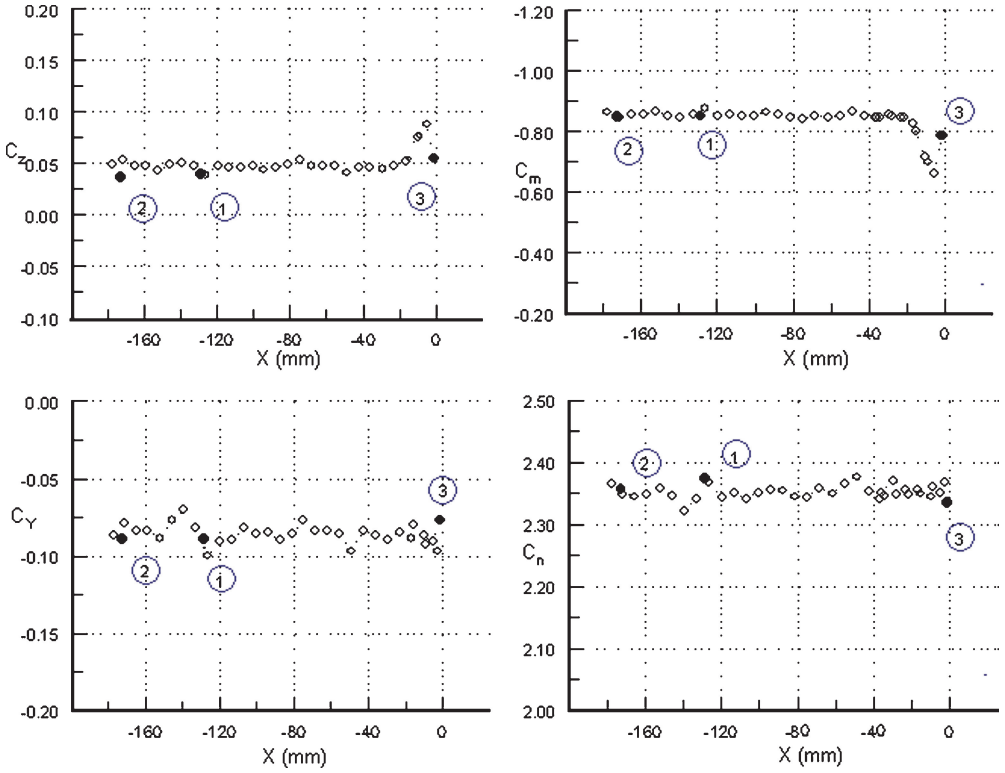


**Fig. 8 MK83-BSU carriage loads for configuration C: $M = 0.95$ and AOA = 2 deg.**

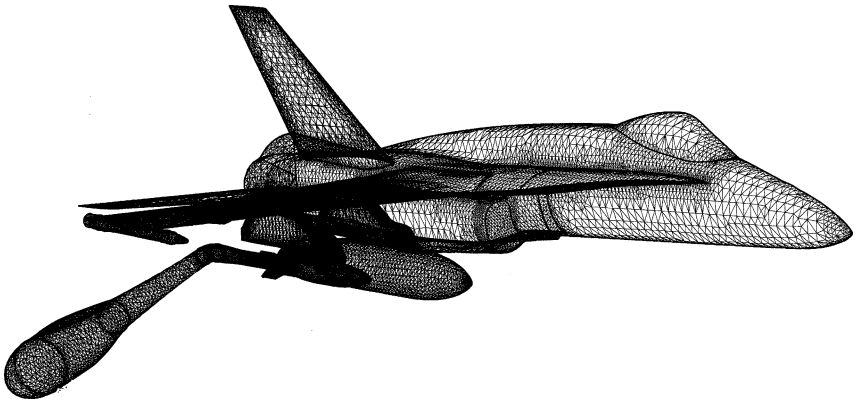

**Fig. 9 Grid of CF-18, pylon, VER, MK83-BSU, and cranked sting.**

For comparison, the scales of load coefficients are kept the same as in Fig. 6. The store loads show less variations with the sting position in the vicinity of the store than in the preceding case; however, the sting-induced increments are nearly the same as those at $M = 0.6$, except for the pitching moment. A large increment of pitching moment, 0.23, is observed, which is higher than that at $M = 0.6$.

In Fig. 8, the store captive loads vs the sting distance for $M = 0.95$ are illustrated. As the sting moves towards the store from about 17.78 cm (7 in.) behind, all of the store force and moment curves remain more or less constant although fluctuations are observed. The variations in magnitudes are much smaller than those at $M = 0.6$ or 0.85. The store captive loads obtained with the sting are essentially the same as those without the sting. The insensitivity of store loads to the presence of the sting is attributed to the fact that the flow is supersonic over the store tail body and the sting behind the store could not influence the flow upstream.

The flowfield around the store at transonic speeds is complicated with the flow characteristics of shock-wave formation and interaction, strong viscous-inviscid interaction, and mutual interference between aircraft components and stores. As stated earlier, the sting-induced store loads vary with aircraft/stores configuration, angle of attack, Mach number, and ratio of the sting diameter to the store base diameter. The present investigation indicates that the sting effects on store loads may not decrease monotonically with increasing Mach number. Detailed analysis is necessary for each individual case if accurate sting effects are required.

## Computational Verification

To supplement the wind-tunnel investigation, a numerical analysis with an Euler code was carried out. The Euler code was developed at IAR and successfully used to predict the F/A-18C/JDAM separation trajectories.[9] The Euler solver was based on Jameson's cell-centered finite volume formulation with the addition of explicit second- and fourth-order artificial viscosity. The boundary conditions on the CF-18 wing and body were satisfied by setting the normal velocity to zero, whereas at the far field a characteristic approach with the Riemann invariants was employed. Special attention was paid to modeling the engine inlet and the effect of engine mass flow ratio. For these computations an inlet mass flow ratio of 0.75 was used.

The unstructured grid of the CF-18, pylon, VER, MK83-BSU and cranked sting (the upstream portion of the articulated sting) for configuration C at AOA = 2 deg is shown in Fig. 9. The pressure

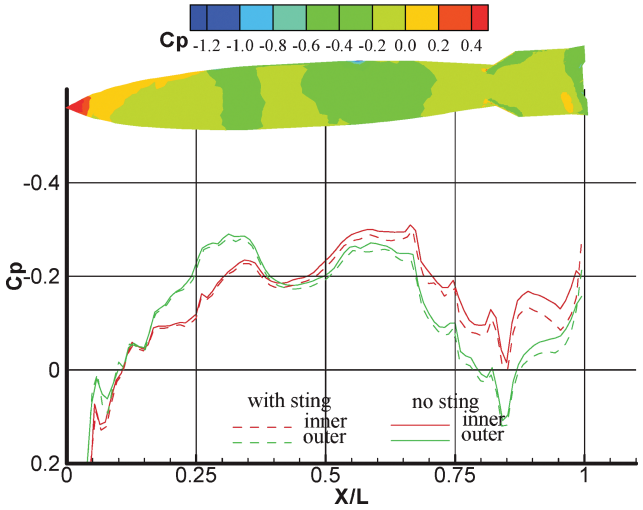


**Fig. 10 Pressure coefficient profiles along store meridian lines: $M = 0.6$.**

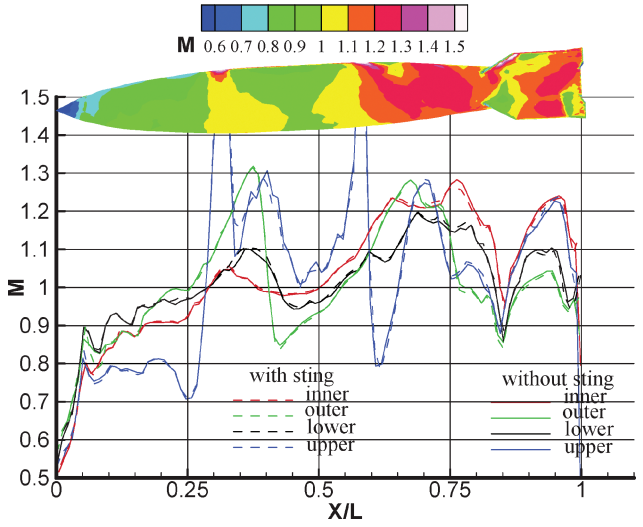


**Fig. 11 Mach-number profiles along store meridian lines: $M = 0.95$.**

coefficient distributions along the inner and outer meridian lines of the MK83-BSU at $M = 0.60$ are illustrated in Fig. 10. Dashed lines are the computed results with the cranked sting attached to the store, while solid lines are results without the sting. Superimposed in the figure is the pressure coefficient contour plot on the store inner surface at the carriage position without the sting. It is found that the pressure on the inner and outer surfaces of the aft portion of the store is increased as a result of the presence of the sting, particularly in the tail region. The total inward side force over the store surface is decreased because of a slightly larger increment of pressure on the inner surface of the store aft portion than that on the outer surface. As a result, the inward side-force coefficient is decreased and so does the yawing-moment coefficient. These are consistent with the wind-tunnel test results in Fig. 6. The similar trends are observed for the normal-force and pitching-moment coefficients at $M = 0.6$. For the case of $M = 0.85$, the sting effects on the store captive loads are similar to those observed at $M = 0.6$.

Variations of Mach numbers along the four meridian lines of the store at a freestream Mach number of 0.95 are shown in Fig. 11. The results with and without the sting are compared, and the Mach-number contour plot on the inner surface of the store without the sting is shown on the top of the figure. Complexity of the flowfield around the store is expected as complicated shock-wave structures and interactions between the store and aircraft components are involved. Detailed analysis of the flowfield is beyond the scope of this paper. However, one thing is clear, that is, over most of the store tail surface the Mach number is greater than 1 and the sting has hardly any effect on the Mach-number distributions. This might explain why the sting has negligible effect on the store captive loads at $M = 0.95$ (see Fig. 8).

## Sting Effects on Separation Trajectories

The ultimate goal of store loads measurements in wind tunnels is to use these data to predict separation trajectories of stores released from their parent aircraft. In this sense, it is worthwhile to assess the effects of the sting support on store separation trajectories and provide some guidelines for store certification work. A store separation analytic model was used to calculate separation trajectories of the MK83-BSU released from the CF-18. This program was developed at Bombardier, Inc., Canadair Division[10] and undergoes continuous upgrade.

The current version of the program can simulate trajectories of powered and unpowered stores ejected from both CF-5 and CF-18 aircraft, in a single-release or ripple-release mode. The code can also simulate aircraft steady heading, banked sideslips, and steady banked turns. The program uses the ejection, aerodynamic, and gravitational forces and moments acting on the store to solve the six-degrees-of-freedom Euler equations of motion and predict store trajectories. The ejection force and moment are acquired from ground-testing results, and the effect of wing deflection as a result of store ejection is considered. The store static freestream aerodynamic coefficients and interference coefficients are obtained from wind-tunnel tests, whereas the aerodynamic damping is obtained from classic literature[11,12] when relevant data are not available.

For the present study, the MK83-BSU interference aerodynamic coefficients at the carriage location were obtained by subtracting the store freestream loads from its captive loads. The MK83 freestream aerodynamic properties were derived from the MK82 data because they are geometrically similar stores. A simple exponential decay of the interference coefficients with the separation distance was assumed. That is, $C = C_0\, e^{-nR}$, where $R$ is the separation distance between the store reference point and the release reference point, $n$ is a constant, and $C_0$ denotes the store captive interference load. The assumption of an exponential or sine decay of store interference coefficients within the aircraft flowfield has been widely accepted in aircraft/store separation prediction.[10,13]

Trajectories of the MK83-BSU released from the CF-18 were analyzed for various configurations, Mach numbers, and aircraft angles of attack. The displacements and Euler angles of a released MK83-BSU relative to the aircraft at $M = 0.6$ and AOA $= 2$ deg for configuration C are shown in Fig. 12. The aircraft was assumed at level flight with an altitude of 6096 m (20,000 ft). The store displacements and Euler angles with the sting effects are compared with those without the sting effects from the moment of release to 0.5 s later. The differences in store displacements are negligibly small, only 1 mm (0.04 in.) in the axial and lateral directions and 4 mm (0.16 in.) in the vertical direction in full scale at $t = 0.5$ s. The corresponding angular discrepancy is 0.5 deg for pitch and 0.8 deg for yaw and roll. In terms of store safety separation, the variations of store displacements and Euler angles during the first 200 ms are more critical. At $t = 0.2$ s, the angular discrepancy is only 0.1 deg in pitch and 0.25 deg in yaw and roll. Similar results are observed in Fig. 13, where the MK83-BSU trajectories with and without the sting effects are compared at the same release conditions except for $M = 0.85$. Because of increasing Mach number, the store axial displacement is increased, and so are the lateral displacement and Euler angles. At $t = 0.2$ s, the errors caused by the sting effects are less than 4 mm (0.16 in.) in store displacements in full scale and less than 1 deg in store Euler angles. For $M = 0.95$, the store trajectories with and without the sting are almost identical as expected, although it is not shown here. The preceding comparisons suggest that in terms of store safety release the sting effects on the MK83-BSU separation trajectories can be neglected for the conditions considered. The main reason is that the ejection force acting on the store is much larger than the aerodynamic loads at the moment of release and therefore dominates the store motions during the aircraft and store separation period.

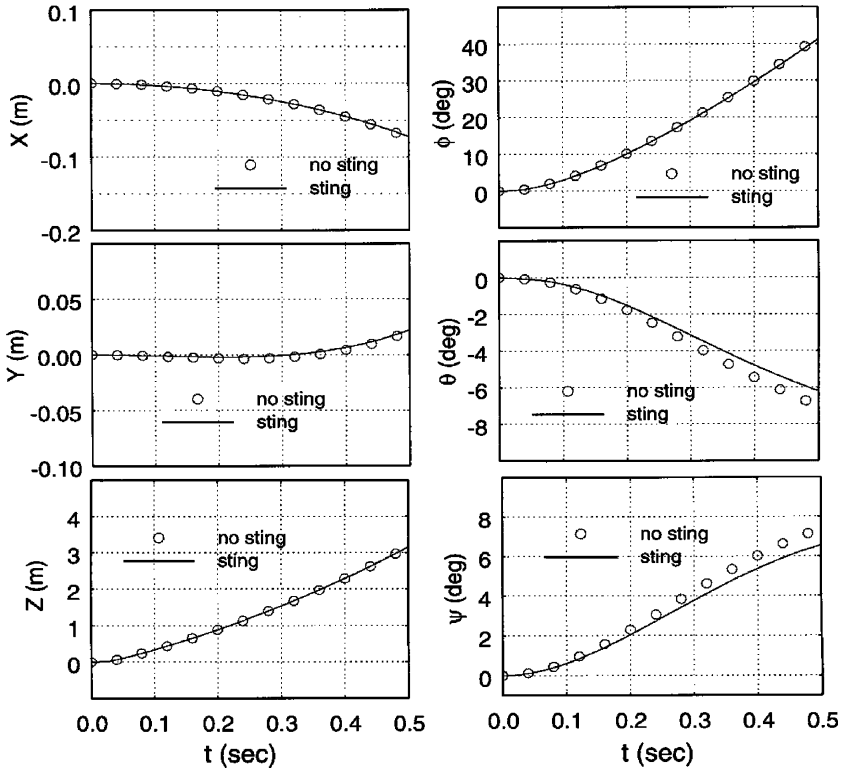


**Fig. 12 MK83-BSU trajectories at AOA = 2 deg, $M = 0.6$, and $H = 6096$ m.**

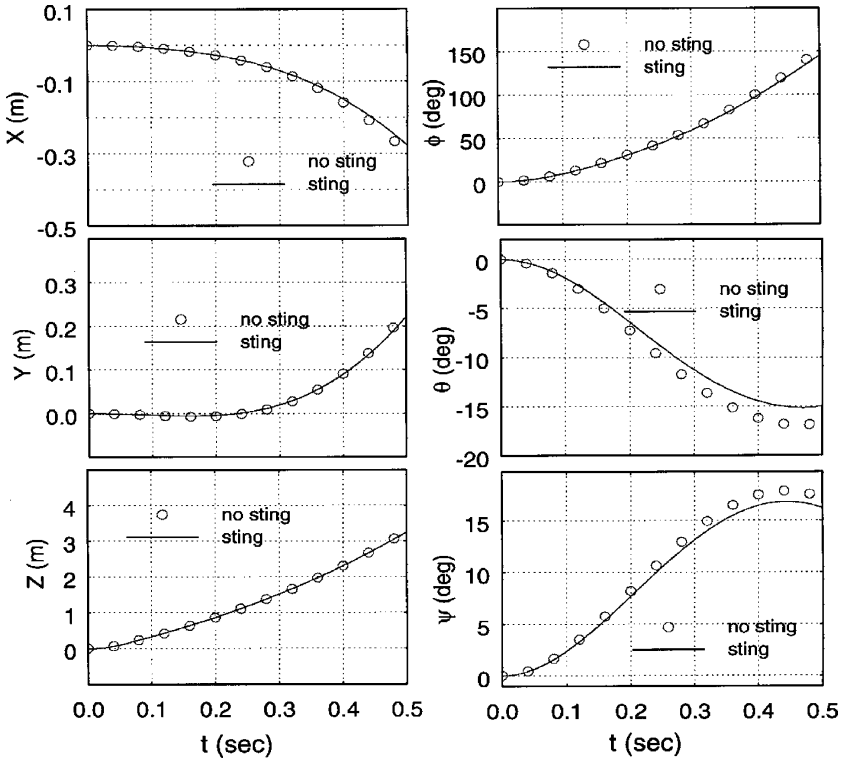


**Fig. 13 MK83-BSU trajectories at AOA = 2 deg, $M = 0.85$, and $H = 6096$ m.**

## Conclusions

The effects of the articulated sting on the captive loads of the MK83-BSU store mounted on a 6% scale CF-18 model were obtained at three Mach numbers, angles of attack, and aircraft/stores configurations. The presence of a sting modifies the flowfield behind the store, alters the pressure distribution on the aft portion surfaces of the store, and thus induces increments in store aerodynamic loads. The wind-tunnel results are qualitatively verified by the computational solutions from an Euler code.

The influence of Mach number on the sting-induced increments in store loads is complicated, particularly at high transonic speeds, and the induced increment may not monotonically decrease with increasing Mach number. A detailed analysis is needed for each individual case if the accurate sting effects are required.

The trajectories of the MK83-BSU released from the inboard of the outboard VER of the CF-18 were predicted with the captive loads measured with and without the sting effects. The errors caused by

the sting interference are negligible for the conditions tested in the release period of interest.

## References

[1]Lynch, F. T., Crites, R. C., and Spaid, F. W., "The Crucial Role of Wall Interference, Support Interference, and Flow-Field Measurements in the Development of Advanced Aircraft Configurations," (Advisory Group for Aerospace Research and Development, North Atlantic Treaty Organization) conf. proceeding, Neuilly sur Seine, France, 1994, pp. 1-1–1-38.

[2]Cahn, M. S., "An Experimental Investigation of Sting Support Effects on Drag and a Comparison with Jet Effects at Transonic Speeds," NACA 1353, June 1958.

[3]Lee, G., and Summers, J. L., "Effects of Sting Support Interference on the Drag of an Ogive-Cylinder Body with and Without a Boattail at 0.6 to 1.4 Mach Number," NACA RM A57I09, Sept. 1957.

[4]Dix, R. E., "Strut Support Interference on a Cylindrical Body with Boattail at Mach Number from 0.6 to 1.4," Arnold Engineering Development Center, AEDC TR-76-40, Arnold AFB, TN, May 1976.

[5]Dix, R. E., "Influences of Sting Support on Aerodynamic Loads Acting on Captive Store Models," Arnold Engineering Development Center, AEDC-TR-76-1, Arnold AFB, TN, March 1976.

[6]Cenko, A., Phillips, K., and Holmes, M., III, "Captive Trajectory System Sting Effects on Store Loads," AIAA Paper 1994-0195, Jan. 1994.

[7]Öhman, L. H., Brown, D., Chan, Y. Y., Galway, R. D., Hashim, S. M., Khalid, M., Malek, A. F., Mokry, M., Tang, N., and Thain, J. A., "New Transonic Test Section for the NAE 5FTx5FT Trisonic Wind Tunnel," National Research Council Canada, NAE-AN-62, Ottawa, Jan. 1990.

[8]Tang, F. C., Jiang, L. Y., and Öhman, L. H., "Transonic Flow Field Around the CF-18 Wing at Angle of Attack 4.5°," AIAA Paper 2000-0797, Jan. 2000.

[9]Fortin, F., Benmeddour, A., and Jones, D. J., "Application of the Canadian Code to the F/A-18C JDAM Separation," AIAA Paper 1999-0127, Jan. 1999.

[10]Kohiyar, F. A., Stathopoulos, N., and Lacroix, A., "CF-18 Store Separation Model AIM-7 Missile Capability," Bombardier, Inc., Canadair Div., RAU-261-158, Canada, Nov. 1995.

[11]Bryson, A. E., "Stability Derivatives for a Slender Missile with Application to a Wing-Body-Vertical Tail Configuration," *Journal of Aerospace Sciences*, Vol. 20, No. 5, 1953, pp. 297–308.

[12]Chin, S. S., *Missile Configuration Design*, McGraw–Hill, New York, 1961, Chap. 9.

[13]Keen, K. S., "New Approaches to Computational Aircraft/Store Weapons Integration," AIAA Paper 1990-0274, Jan. 1990.